Current Based HVAC Systems Air Filter Diagnostics and Monitoring

Fadi M. Alsaleem
Wichita State University, United States of America, fadi.alsaleem@wichita.edu

Michael Munroe
Emerson Climate Technologies,United States of America, michael.munroe@emerson.com

Mostafa RAFAIE Rafaie
Wichita State University, United States of America, mostafa.rafaie@gmail.com

Current Based HVAC Systems Air Filter Diagnostics and Monitoring

Fadi ALSALEEM[1]*, Michael MUNROE[2], Mostafa RAFAIE[1]

[1]Wichita State University, Department of Mechanical Engineering,
Wichita, Kansas, USA
Contact Information (316-518-5825, mxhhasan@wichita.edu)

[2]Emerson Climate Technologies, Residential Solution
Sidney, Ohio, USA
Contact Information (937-494-7874, Michael.Munroe@Emerson.com)

* Corresponding Author

ABSTRACT

This paper addresses the use of continuous indoor motor current to detect filter blockage in HVAC system. A commonly known phenomenon exists in the loading of a typical indoor motor blower that results in a power consumption decrease and hence less current draw for PSC motor, and power and currant draw increase for constant torque motor. Testing using Akaike information criterion (AIC), classification and regression tree (CART) models, and using both fixed radius basis function and linear basis function was described and performed against field of installed systems to determine if candidate data filter was sufficient, or to motivate use of Mann-Kendall to determine trend existence, strength, and transition in existence or strength. The bases, commonly used in practice, were found to have cumulative effectiveness against only 50.4% of installed systems, and were strongly differentiated in performance against motor type. The Mann-Kendall approach was found to have performance of ~88% of evaluated systems. This approach calculates the confidence trending level corresponds to the nonparametric correlation coefficient for the indoor current daily averages. Trend levels will be accumulated over time and will be used to declare filter blockage once they suggest a strong trend in the direction of filter blockage.

1. INTRODUCTION

Most heating, ventilation, and air-conditioning (HVAC) systems in commercial buildings and residential homes are equipped with air filters to improve indoor air quality. Filter is intended to be used to collect dirt, debris, and dust and prevent their accumulation anywhere else. To prevent excessive dirt accumulation and possible HVAC performance degradation and malfunction, air filters need to be replaced once in periodically. The problem is that there is wide variation, even in the nearby houses, in the rate of accumulation of debris in the air filter. This can be driven by pets, by construction (infiltration rate), or by exposure. Current manufacturer recommendation a replacement of air filter every 3 months per inch of filter. While this approach minimizes the worst case, it also allows the inference with uniform rate of deposition, that one average day of use consumes less than an average of about 1.1% of filter capacity. In this work, however, we developed a framework to warn the need for filter replacement based on scientific data rather using the 3 months rule.

The impact of filter quality and its current conditions on HVAC system performance has received great deal of attention in the literature. For example, Yang et al. (2007) studied this impact using different filter types (six different level of filtration) on three different HVAC systems. Two series of tests were performed while the filters are in healthy and dirty states. The study showed that a dirty filter could cause significant reduction in HVAC cooling capacity, increase in the pressure drop across the filter, and increase in the indoor fan power usage. Another study (Stephens et al., 2010) was performed on a residential home in Austin, Texas. While the HVAC system energy use was monitored, different filters MERV (MERV < 4, MERV 8. and MERV 11) were tested in two different HVAC systems. The study shows that energy consumption increases with dirty filter but did not differ much with high-efficiency filters compared to low-efficiency filters.

2. DIRTY FILTER DETECTION ALGORITHMS

2.1 Hardware and Experiment Set-up

A sample of 225 HVAC systems that are installed in real homes were used in this investigation. Of these systems, 118 were charged with R410A refrigerant and the rest were charged with R-22 refrigerant. The tonnage size and SEER information for this sample size is given in Figure 1. The hardware that is used to collect data from these systems is shown in Figure 2 and is described in extensively in (Alsaleem et al., 2016). Few key points are to be mentioned about the hardware. (1) It consists of an indoor kit that is equipped with voltage and current sensors as well as temperature sensors to track air supply, air return, indoor liquid line, and suction line temperatures. The outdoor kits measure the aggregate outdoor current and voltage. (2) the data for each system run is transmitted in chunks, each of fifteen minutes maximum length and at sampling rate of one sample per five seconds (0.2 HZ),(3) a cloud structure is built to host algorithms to receive and processes the data from the indoor and outdoor kits.

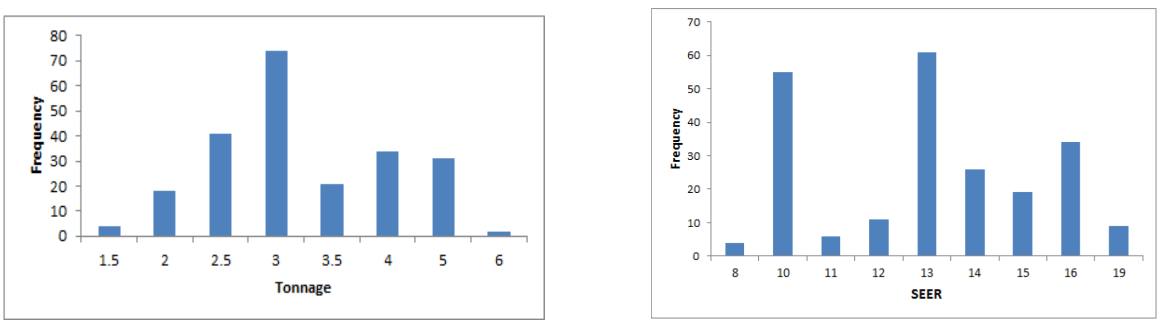

(a) (b)

Figure 1: The tonnage size (a) and SEER ratting (b) for the 225 HVAC systems used in this study

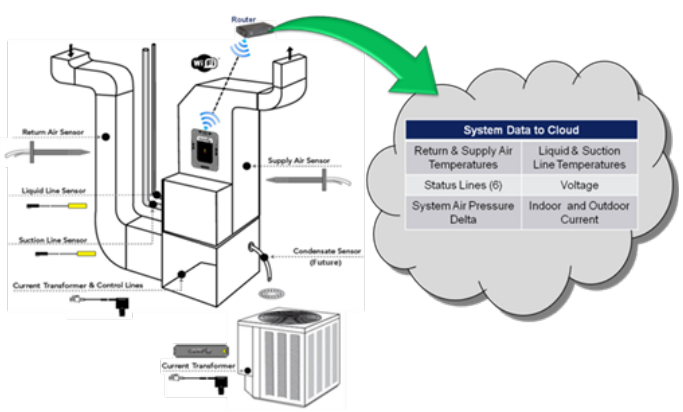

Figure 2: Hardware shows the indoor and outdoor kits to gather and send sensors data to the cloud

2.2 Dirty Filter Detection Basic Idea

A commonly known phenomenon exists in the loading of a typical indoor motor blower that results in a power consumption decrease for PSC motor and power increase for constant torque motor. A dirty filter-detection algorithm benefits from this simple fact to capture filter blockage over time by monitoring the daily averaged indoor motor power. Figure 3(a) illustrates the normalized daily average of the indoor current of one of the filed monitored HVAC system correlated to the expected airflow percentage drop as the filter developed dirt over time. The figure demonstrates that filter degradation over time can be detected only by using current measurement. This chart also shows the time when the homeowner changed the filter, by the sudden jump by the end of September. Figure 3(b) visually confirms the predicted poor filter performance before replacement.

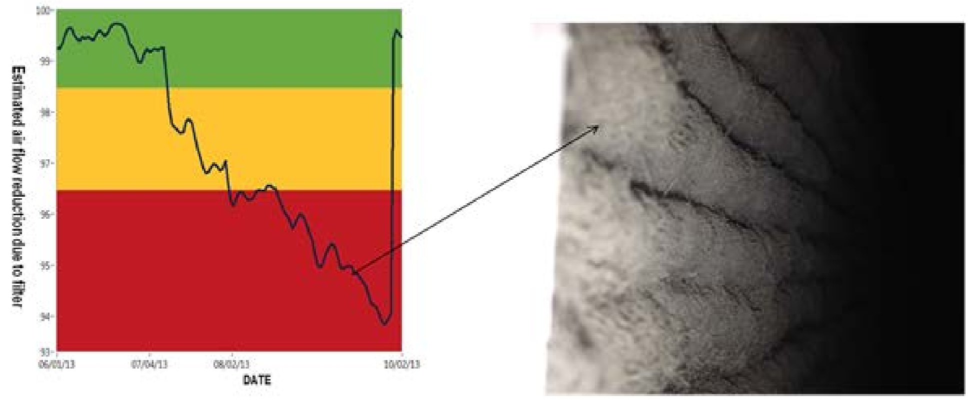

(a) (b)

Figure 3: Indoor current correlation to filter blockage, (a) data of the normalized indoor current over time correlated to the airflow reduction, (b) the dirty filter before replacement.

In order to reduce the effect of special cause variation on disposition some level of signal conditioning precedes analysis. The major axes of variation in indoor current measurement are going to include run-to-run, solar hour-of-day, week-of-year, by year, conditioning-mode (AC/HP, number stages, etc.), by indoor temperatures (wet and dry bulb), by equipment make/model/manufacturer, by installed configuration, by installer and installation, by home size/insulation/exposure, by geographic location, by maintenance history, by operation history, and by current homeowner configuration and operation. The following examples are around air filter health, so the variables most strongly related to that are considered.

Common types of variation that confound with air filter indication include variation of load by hour of day, by indoor temperatures, by operation (count of stages) and by changes to configuration including occlusion of returns or changes to registers by the homeowner. The first is accounted for by averaging across a full day, including both daytime and nighttime use. The second is accounted for using normalizations like using historic data to approximate the relationship between indoor current and indoor temperature as a polynomial. The third can be accounted for by tracking control signal. The fourth has the challenge that there is no leading variable, and that it is a discontinuous jump. On either side of the discontinuity, the polynomial relationship between power and time is consistent, and acts as if one added a scaled unit step at that point in time. When there is a fundamental change, such as a replacement of a dirty filter with a clean one, the coefficients of the polynomial, after accounting for the jump, change in a sustained manner.

2.3 Linear and Redial Fitting Approaches

Two simple but effective bases for “appropriate function” to model filter behavior over time included fixed variance radial clustering (a cousin of k-means), and purely linear least squares fit. The assumption of the constant diameter radial model is that jumps outside the “radius” were not indication of filter behavior. The background, derivation, and proper use AIC or corrected AIC as used herein is more comprehensively described in (Akaike, 1992).

The “Information Criteria” measures of fit are derived from Kullback-Leibler divergence and via approximations for log-likelihood, and account not only for error as R^2, but model complexity and sample size. One condition of use to compare two or more models is that the same data must be used for all model evaluations. A lower value of criteria is indicative of higher likelihood. The AIC was used to compare the performance of radial clustering and linear fitting.

The expressions for AIC used in this work was:

$$AIC = n \cdot ln\left(\frac{RSS}{n}\right) + 2 \cdot k \tag{1}$$

Where “RSS” is the residual sum of squares (or sum of squared error), “n” is the number of observations, and “k” is the number of parameters in the model. Each split was considered a piecewise Heaviside function, so it has only the parameter of the location of the split plus the sum of parameters of the fit-model within each split. A three term linear expression would then be described as:

$$Amps(t) = (linear1 + H(t_1) * linear2) \cdot \left(1 - H(t_2)\right) + H_2 \cdot linear3 \tag{2}$$

This expression has two parameters for each linear expression and the two parameters for the two Heaviside functions for a total “k” value of “8”. Number of samples was large enough that correction was not required in this case.

A Classification and Regression Tree (CART) model was used to evaluate performance of these for ability of the basis to account for jumps by testing non-split then split transformations for AIC. In another words, as sudden jump in indoor current are expected to happen, the CART model will be used to remove the effect of jumps in the accuracy. The premise of the CART is that the leaf-tip is constant, and splitting can be single axis at a time to improve either GINI coefficient or accuracy. While the CART premise is incompatible with detection of slope, the greedy splitting is optimal for detection of univariate jumps. In analogy to nontransitive dice, while this CART approach is inadequate for directly filtering the data, it is sufficient for evaluation of the filtering algorithms. While a full discussion of CART models is substantially beyond the scope of this text, there are excellent references including (Breiman et al 1984).

If the CART imposed splits improved the AIC by a factor less than 2.198, then the basis was deemed "capable" otherwise, it was deemed "incapable". This means that if the CART imposed splits did not make the old model contain any less than 25% of the weight, then the old model was considered "capable". This balanced, non-greedy approach to the setting of the weight threshold was made in consideration of the technical confidence of high levels of noise in the overall system and using the game-theoretic idea of "equal division of the contested value" (Talwakar 2014).

The log of the likelihood of a model given a difference in AIC compared to a model with minimum AIC is negative one half the difference; the weight for addition of models is the likelihood of the individual divided by the sum of likelihoods in the ensemble and the constant of proportionality divides out. A delta AIC of 5.882, as can be seen in Table 1, indicates a relative (Akaike) weight below 5%. Table 1 indicates a few common AIC thresholds and weight, and then indicates common weights and their thresholds, for 2-component weighted mixture of models.

Δ AIC	Weight		Weight	Δ AIC
0	50.0%		33%	1.416
0.5	43.78%		25%	2.198
1	37.75%		10%	4.395
2	26.89%		5%	5.889
3	18.24%		1%	9.191

Table 1: Useful list of values relating difference in AIC with component weight in additive model when there are two components under consideration.

It was found, using the above criteria, that the linear was capable for 39.0% of 225 HVAC systems and not capable for 61.0% of them. Similarly, the radial approach was capable for 27.5% of systems but was incapable for 72.5% of them, the details of these calculation are beyond the scope of this paper and will be discussed in a separate work. When combined they were capable for 50.4% of all systems. These very simple bases, while easy in practice to execute, are substantially incapable of handling the naturally occurring variation. This motivates the use of the Mann-Kendall test.

For the remainder of this section, we first review the Mann-Kendall test, and then discuss the trending analysis use in warning of dirty filter.

2.4 Mann-Kendall Trending Test

The purpose of the Mann-Kendall test is to assess for a given data if there is a monotonic trend over time. It has been used in many applications, such as water quality monitoring (McLeod et al., 1990) and more recently for weather trending and prediction (Soltani et al., 2013). Its advantages over linear regression approach include it does not require a normal distribution for the data, it is independent of the data magnitude, and it can deal well with missing or irregularly spaced data. The trending test compares each data point to all subsequent values. If the data from newer values is greater than earlier data, then the Mann-Kendall statistics value S is increased by 1.0; otherwise, it decreased by 1.0. In mathematical terms, this could be described as:

$$S = Sign\left(\sum_{i=1}^{m-1} \sum_{j=i+1}^{m} \begin{cases} 1\ if\ (T_j - T_i) > 0 \\ 0\ if\ (T_j - T_i) = 0 \\ -1\ if\ (T_j - T_i) < 0 \end{cases} \right) \tag{3}$$

where T_i, T_j are the daily average values for a given measurement at a given day where j > i. A very high positive S value indicates an increasing trend, whereas a very low negative value indicates a decreasing trend. The sign function, introduced by the authors, adjusts the sign of the S value to always indicate a positive value if the measurement trend direction support the fault.

To account for sample size, the magnitude of *S* was adjusted by the following scale (assuming sample data are not similar) as follow *(*HydroGeoLogic, 2004*)*:

$$S_N = \frac{S \mp 1}{g(S)^{1/2}} \tag{4}$$

where, $g(S) = \frac{1}{18}[n(n-1)(2n+5)]$, and *n* is the sample size.

Mann-Kendall use for dirty filter detection

Figure 4 shows a flowchart for the algorithm of performing the Mann-Kendall to detect dirty filter. The process starts when the filter detection algorithm receives a new daily average for the indoor motor current data. Next, the algorithm adds the data to the existing dataset of previous data and applies the Mann-Kendall analysis described above. Based on the Mann-Kendall analysis, the algorithm calculates the trend confidence level, in the range of -1 to 1. The trend confidence level corresponds to the nonparametric correlation coefficient (S_N) described above.

The algorithm scales the estimated value based on duration in time of the new data set and then adds it to a cumulative sum. The scaling is based on the time duration represented by the current data sample being added to the data set versus the time duration represented by the existing data set of previous data. For example, a confidence level corresponding to one week will be appropriately scaled or weighted when added to, for example, previous data corresponding to six weeks. Next, the algorithm determines whether the absolute value of the trend confidence sum is greater than a predetermined threshold. In this implementation, the predetermined threshold used is 2.0. This value was chosen based on correlation analysis between the empirically confirmed amounts of dirt for multiple filled and dirty filters to the absolute trend sum. When the absolute value of the trend confidence sum is greater than 2.0, the algorithm generates a dirty filter alert, resets the trend confidence cumulative to 0.0, and loops back to starts the trend analysis again. On the other hand, if the absolute value of the trend confidence sum is less than 2.0, the algorithm applies a new filter detection algorithm. In this case, the algorithm determines whether the current data is within three sigma (standard deviation) of the average data over time. When the current data is not within three sigma of the average data, and has stayed outside of three sigma of the average data for a predetermined duration of two days, the algorithm determines that the filter has been replaced and generates a new filter acknowledgment and resets the trend confidence sum to 0.0.

With reference to Figure 4, a graphical representation of using the Mann-Kendall algorithm, depicted in the flowchart of Figure 5, in warning of dirty filter is illustrated for a sample unit data. Figure 5(a) shows a plot of daily averages of indoor blower fan current over time in which each square represents one full day's average value. Similar to Figure 5(a), the plot indicates that the filter has been replaced with a new filter when the current spiked from 6.05 Amp to 6.50 Amp, seven days before the last recorded day average. Figure 5(b), shows a plot of the trend confidence levels, calculated using the Mann-Kendall analysis for the data of Figure 5(a), over time. As depicted in the figure, the trend confidence level is generally a negative number, indicating a downward trend, until the last trend confidence level, when the trend confidence level moves to a positive level, corresponding to the filter being replaced with a new filter.

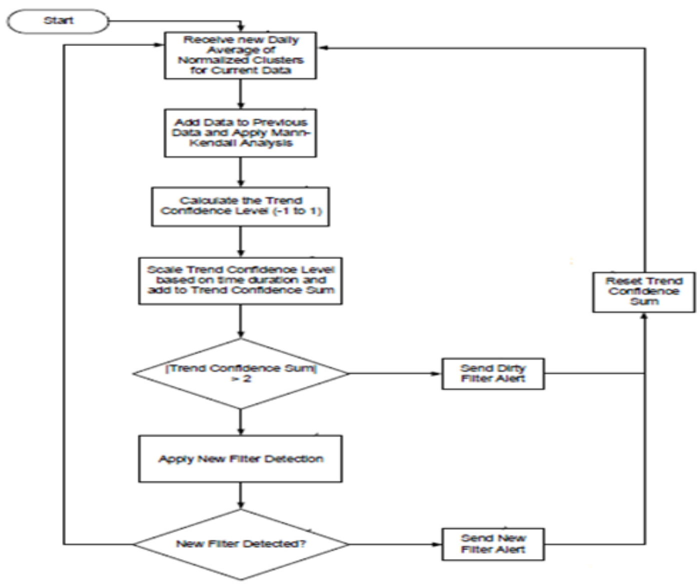

Figure 4: Flowchart for using the Mann-Kendall of warning dirty filter

At Figure 5(c), a graphical representation of the trend confidence sum over time is shown. As shown in the figure, the time interval for which each trend confidence sum is made generally corresponds to the width of each step in the graph. However, the trend confidence sum can be updated more frequently, or less frequently, as desired. The figure shows that the trend confidence sum increases in negative magnitude until it reaches a point at which the trend confidence absolute sum is greater than the predetermined threshold, which in this case is 2.0. With the trend confidence absolute sum greater then 2.0, a dirty filter alert is generated, and the trend confidence sum is reset to *0.0*. The trend confidence sum again begins to increase in negative magnitude, until it reaches the point when the homeowner finally responded to the alert and changed the filter. The algorithm detected this filter change event and the trend confidence sum is reset to *0.0*. The logic to detect the need for a new filter is built to search for a sudden change in the trend with a direction opposite to the normal direction of filter dirt development. Specifically, a moving average of the standard deviation for the indoor current is calculated. If at any given time the current measured value jumped from the previous day value a threshold of at least three times the current averaged standard deviation, then this is reason for a potential reset. If the values for at least three new days in a row still deviate by that threshold, then a trend reset is triggered. The three-day condition is to eliminate a false reset trigger due to measurement noise.

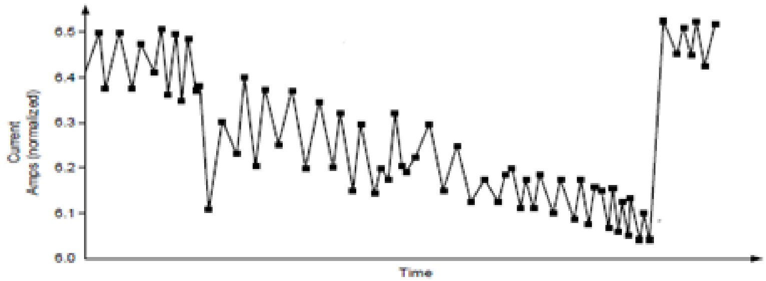

(a) Daily averaged indoor current

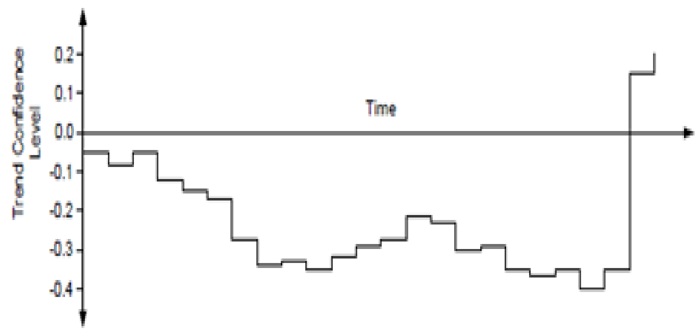

(b) Trend confidence level

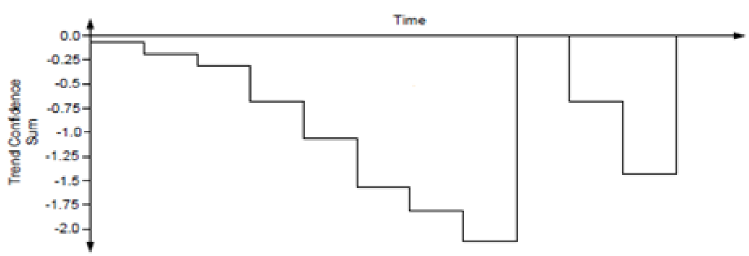

(c)Trend confidence sum over time

Figure 5: A graphical representation of using the Mann-Kendall based algorithm, depicted in the flowchart of Figure 4, in warning of dirty filter for a sample unit, (a) is the indoor current daily average values over time, (b) is the corresponding trend confidence level using the Mann-Kendall test, (c) is the trend sum that is used to compare with a predetermine threshold for potential filter alert.

3. RESULTS AND DISCUSSION

Figure 6 show results for the application of the Mann-Kindle algorithm over the daily averaged indoor current of a HVAC system for more than a year. The system has a PSC motor type. In the figure, the averaged current is in white, the weekly based trend measure is in green, the weekly trend sum accumulation is in red, and the actual filter replacement signal is in blue. The figure demonstrates the idea of using trends confidence level sum to trigger the dirty filter alert. As shown in the figure, the filter alert is triggered if the trend sum exceeds a threshold value of -2 or its mutiples. These events are marked by purple arrows. In average, the filter alert for this system is triggered for at least 1 time per two months. The trend sum accumulation is only rested to zero if the algorism detect a new filter replacement.

The charts in Figure 7 show the filter alerts status generated in a month for the 225 systems. The filter alerts status were obtained from homeowners responses to an online survey, immediately sent after receiving the filter alert. The survey responses reveal that 88% of the filter alerts were valid. System with electrostatics filter is among the highest population for invalid filter alert. Due to the unique dynamics for dirt accumulation and its effect on indoor current, a different algorithm might be needed to tackle electrostatics filter.

Figure 6: Results for the application of the Mann-Kindle algorithm over the daily averaged indoor current of a HVAC system for more than a year

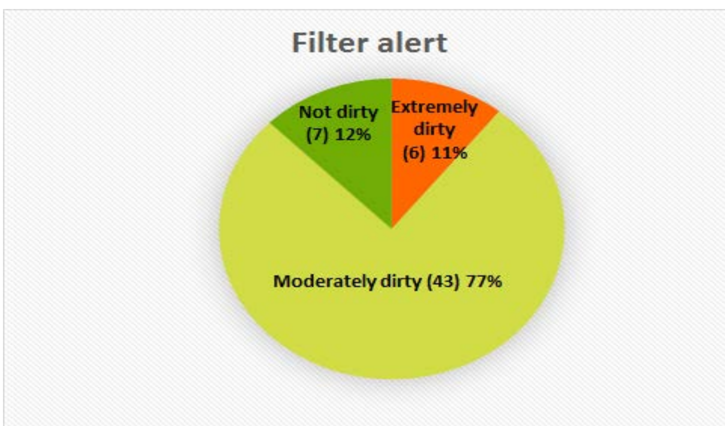

Figure 7: Trending filter alert statistics

4. CONCLUSIONS

This paper addressed the use of continuous indoor motor current to detect filter blockage in HVAC system. Different filter-detection algorithms were designed to capture filter blockage by monitoring the daily averaged indoor current over time. 225 HVAC field units were used in this investigation. An indoor kit that is equipped with current sensor was used to transmit these units' data for each system run in chunks, each of fifteen minutes maximum length and at sampling rate of one sample per five seconds (0.2 HZ). For the candidate models within the duration of the analysis, the Mann-Kendall approach was found to be sufficient for alerting dirty filter. The accuracy of this approach can be further enhanced by combining the trends of other indoor measurements such as the split and evaporator suction temperatures.

REFERENCES

Akaike, H. (1992). Information Theory and an Extension of the Maximum Likelihood Principle. *Springer Series in Statistics*, Perspectives in Statistics. Springer-Verlag: New York, pp. 610-624.

Alsaleem, F., Abiprojo, R., Arensmeier, J., &Hemmelgarn, G. (2014). HVAC System Cloud Based Diagnostics Model, *International Refrigeration and Air Conditioning Conference*, Paper No. 2496, West Lafayette, IN.

Alsaleem, F., &Quedan, A., (2016). Low Refrigerant Algorithm Detection for Cooling Systems Relying on Trending and Data Analysis, to be presented in the 4th *International High Performance Buildings Conference at Purdue*, West Lafayette, IN.

Alsaleem, F., (2015) Current based air filter diagnostics and monitoring, *USA pending patent application* (14/709658)

ASHRAE Standard, (1987). 41.2, Standard methods for laboratory air-flow measurement. A*merican Society of Heating, Refrigerating and Air-Conditioning Engineering*, Atlanta.

ASHRAE Standard, (1986). 41.1Standard method for temperature measurement. *Trans. of the ASHRAE*.

ASHRA E Handbook, (1996). HVAC systems and equipment. *Trans. of the ASHRAE*

Breiman, L., Friedman, J., Olshen, R., and Stone C., (1984). Classification and Regression Trees. Belmont, California: Wadsworth.

Deru, M., Field, K., Studer, D., Benne, K., Griffith, B., Torcellini, P., and Yazdanian, M. (2011). US Department of Energy *commercial reference building models of the national building stock*

Hipel, K.W. & McLeod, A.I. (1994). Time Series Modelling of Water Resources and Environmental Systems, Amsterdam: *Elsevier*. ISBN:0-444-89270-2.

Hirsch, R.M., Slack, J.R. & Smith, R.A. (1982). Techniques for Trend Assessment for Monthly Water Quality Data, *Water Resources Research*, vol.18, P.107-121.

HydroGeoLogic, Inc. (2004). Annual Groundwater Monitoring Report – *Former Fort Ord*, California.

Montgomery, J. F., Green, S. I., Rogak, S. N., & Bartlett, K. (2012). Predicting the energy use and operation cost of HVAC air filters. *Energy and Buildings*, vol. 47, 643-650.

Nassif, N. (2012). The impact of air filter pressure drop on the performance of typical air-conditioning systems. *In Building Simulation* (vol. 5, No. 4, pp. 345-350). Tsinghua Press.

Priotomo, R., and Alsaleem F., (2015) HVAC system air filter diagnostics and monitoring, *USA pending patent application* (14/712049).

Soltani, M., Rousta I., & Modir T. (2013). Using Mann-Kendall and Time Series Techniques for Statistical Analysis of Long-Term Precipitation in Gorgan Weather Station, *World Applied Sciences Journal*, vol. 28, no. 7, pp. 902-908.

Stephens, B., Novoselac, A., & Siegel, J. A. (2010). The effects of filtration on pressure drop and energy consumption in residential HVAC systems (RP-1299). Hvac&R Research, vol. 16(3), 273-294.

Talwalkar, P. (2014). The joy of game theory. *CreateSpace Independent Publishing Platform*, pp. 32-39.

Yang, L., Braun, J. E., & Groll, E. A. (2007). The impact of evaporator fouling and filtration on the performance of packaged air conditioners. *International Journal of Refrigeration*, vol.30 (3), pp.506-514.